Available online at www.sciencedirect.com
ScienceDirect
Journal of the European Ceramic Society 32 (2012) 409–418
www.elsevier.com/locate/jeurceramsoc

Influence of brick pattern interface structure on mechanical properties of continuous carbon fiber reinforced lithium aluminosilicate glass–ceramics matrix composites

Long Xia, Xinyu Wang, Guangwu Wen *, Xia Li, Chunlin Qin, Liang Song

School of Materials Science and Engineering, Harbin Institute of Technology at Weihai, Weihai 264209, PR China

Received 18 December 2010; received in revised form 27 July 2011; accepted 6 August 2011
Available online 3 September 2011

Abstract

Continuous carbon fiber reinforced lithium aluminosilicate glass–ceramic matrix composites have been fabricated by sol–gel process and hot pressing technique. The results show that the Cf/β-eucryptite composites hot pressed at 1300 °C and Cf/β-spodumene composites hot pressed at 1400 °C form weak interface with brick pattern characteristics, leading to high mechanical performance. The maximum flexural strength and fracture toughness reach 571 ± 32 MPa and 9.8 ± 0.6 MPa $m^{1/2}$ for Cf/β-eucryptite composites and 640 ± 72 MPa and 19.9 ± 1.8 MPa $m^{1/2}$ for Cf/β-spodumene composites. On increasing the hot pressing temperature, the active chemical diffusion consumes brick pattern interface layer, which leads to the formation of strong bonding between carbon fiber and the matrix. As a result, the composites exhibit brittle fracture behavior and the mechanical properties decrease significantly.

Keywords: Sol–gel processes; Composites; Mechanical properties; Glass ceramics

1. Introduction

Lithium aluminosilicate (LAS) glass–ceramics, one of the most important glass–ceramics systems, has been extensively investigated over the past several years owing to its ultra-low or even negative coefficient of thermal expansion (CTE) as well as the excellent electrical properties.[1–4]

The applications of lithium aluminosilicate glass–ceramics as high performance materials are severely hindered by their brittle nature. Numerous attempts have been made to improve the toughness of these materials by incorporating fibers or whiskers.[5–9] Compared with the monolithic LAS matrix, carbon fiber (Cf) reinforced glass matrix composites have demonstrated a wide range of attributes including high strength, high stiffness, excellent toughness, low density and unique wear resistance for structural application.[10–13] Moreover, the axial CTE of carbon fibers is nearly zero, which makes them suitable reinforcements in fabricating composites with zero CTE in one dimension. Therefore, Cf/LAS composites can be utilized as ultrastable materials that are required in a wide range of precision devices and instrument equipment in high-tech systems in microelectronics or optical precision applications, such as ring-laser gyroscope and optically stable platform. Cf/LAS composites with high flexural strength and fracture toughness can also be used as substitutions of structural materials, where low or even negative thermal expansion is necessary, such as ZrW_2O_8[14,15] and lithium aluminosilicate[16–18] ceramics.

Densification of the ceramic matrix and control of the interface between the fiber and the matrix are vital in the production of composites with high mechanical performance.[19,20] Conventionally, continuous fiber reinforced lithium aluminosilicate glass–ceramics matrix composites have been fabricated mainly by slurry infiltration method, where the lithium aluminosilicate glass–ceramics matrix was produced by melting the mixture of Li_2O, Al_2O_3, SiO_2, TiO_2 and ZrO_2 powders. However, processing temperature that are as high as 1600 °C and a lengthy sintering time over 4 h are needed to obtain homogeneous LAS glass monolithic.[21–26]

* Corresponding author. Tel.: +86 451 86418860; fax: +86 451 86413922.
E-mail addresses: g.w.wen.hit@gmail.com, g.wen@hit.edu.cn, wgw@hitwh.edu.cn (G. Wen).

0955-2219/$ – see front matter © 2011 Elsevier Ltd. All rights reserved.
doi:10.1016/j.jeurceramsoc.2011.08.021

Table 1
Typical properties of carbon fiber.

Diameter (μm)	Density (g/cm^3)	Tensile modulus (GPa)	Tensile strength (MPa)
6-8	1.78	200–260	3500

A lower crystallization temperature of 800 °C can be achieved by molecular-scale mixing of alkoxide precursors.[27,28] Zhien et al.[29] prepared Cf/LAS composites using LAS sol infiltration and hot pressing method. LAS sol were synthesized by mixing tetraethoxysilane, titanium butoxide and Li, Mg, Al (and Zn) inorganic salts. Nevertheless, it is difficult to control hydrolysis and polymerization of different metal alkoxides due to their different hydrolysis rates. As a result, obtaining the sol with ideal viscous, which is a key factor in preparation of LAS composites by sol–gel route, is difficult to accomplish. In addition, different hydrolysis rates of individual alkoxides may result in chemical inhomogeneity that leads to higher crystalline temperature or to the formation of undesired crystalline phases.[30,31]

The fiber–matrix interface crucially determines the final properties of composite materials. For this reason, the fiber–matrix interface has been the subject of numerous investigations and attempts at optimization. However, most of studies focused on the interface of Nicalon SiC fiber reinforced ceramics matrix composites.[32–36] There is little investigation on the interface characters of carbon fiber reinforced glass ceramics.

In this paper, an improved sol–gel technique for the fabrication of 1D Cf/LAS composites is described. The resultant lithium aluminosilicate sols have controllable viscosities and the problem that different hydrolysis rates of metal alkoxides has been resolved in this system. The matrices were β-eucryptite and β-spodumene. The microstructures of the composites were characterized by X-ray diffraction (XRD) and scanning electron microscopy (SEM). The fiber–matrix interfaces of the composites were examined by high resolution transmission electron microscopy (HRTEM). The thermal stability of Cf/LAS composites was characterized by DTA–TG. The relationship between microstructure and mechanical properties of the composites was discussed in detail.

2. Experimental procedure

2.1. Preparation of composite

The carbon fibers used in this study (Guangwei Industries, Inc. China) have a diameter of 6–8 μm, and its properties are summarized in Table 1. LAS sol in the form of β-eucryptite (Li_2O–Al_2O_3–$2SiO_2$) and β-spodumene (Li_2O–Al_2O_3–$4SiO_2$) were synthesized following a sol–gel method by starting with mixing boehmite sol, silica sol and lithium salt, using deionized water as media. The slurry was prepared by adding methyl cellulose into the LAS sol. The prepreg was prepared by infiltrating the continuous carbon fiber into the as-prepared slurry and drying. Unidirectional carbon fiber reinforced lithium aluminosilicate glass ceramics matrix (1D-Cf/LAS) composites were prepared by stacking the prepreg into a graphite mould and hot-pressing with 10 MPa at different temperatures under vacuum condition. The content of carbon fiber was approximately 35–40 vol.%. The prepared composites were denoted as Cf/LAS2 and Cf/LAS4, corresponding to β-eucryptite and β-spodumene matrix respectively.

2.2. Evaluation of mechanical properties

Bulk densities of the samples were measured with deionized water as immersion medium according to the Archimedes principle. The flexural strength was measured by three-point-bending tests on 3 mm × 4 mm × 36 mm bars at a cross-head speed of 0.5 mm min^{-1} and a span of 30 mm. The value of the flexural strength was calculated as:

$$\sigma_f = \frac{3PL}{2bd^2} \quad (1)$$

where P is the maximum applied load, b is the width, d is the specimen thickness, and L is the span of the bending specimen. Single-edge-notched-beam (SENB) test was used to assess the fracture toughness with a cross-head of 0.05 mm min^{-1} and a span of 20 mm. The samples were 2 mm × 4 mm × 20 mm with a notch depth to sample thickness ratio of 0.5, and the notch was made in the plane normal to the fiber layers.

2.3. Characterization of microstructures

The microstructure observation and composition analysis were carried out in transmission electron microscope (TEM, JEM-2010, Jeol, Japan) equipped with energy-dispersive X-ray spectrometer (EDX). In addition, the fracture surfaces of the samples were observed by a scanning electron microscopy (SEM, Vega II, Tescan, Czech), and the phases in the samples were identified by X-ray diffractometer (XRD, D/max-γB, Rigaku, Japan).

The crystal morphologies and crystal size of Cf/LAS composites were analyzed by SEM. Polished specimens were etched in 5 vol.% HF solution for 60 s. The major crystal phase was observed because glass phase was dissolved in HF solution.

2.4. Residual tensile strength of carbon fibers

The carbon fibers in the Cf/LAS composites sintered at different temperatures were obtained by immersing the composites into 40 vol.% HF solutions for 48 h, where the lithium aluminosilicate matrix dissolved into the HF solutions and the carbon fibers exposed. Single fibers were manually separated from fiber bundles and glued onto a paper frame. Tension tests were carried out on an electromechanical tensile machine equipped with mechanical grips. During mounting, the specimens were handled only by the paper frame. Upon clamping of the ends of the paper frame by grips of the test machine, both sides of the frame were carefully cut in the middle. The tests were displacement controlled with the loading rate of 1 mm min^{-1} and a gauge length of 20 mm. Fig. 1 shows tensile specimens and their loading modes of the carbon fiber. To avoid any damage to

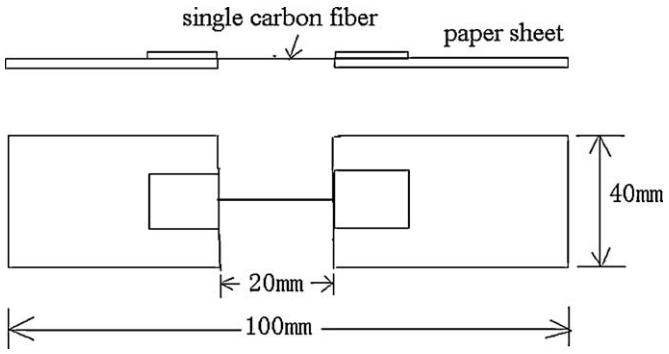

Fig. 1. Diagram of tensile specimen.

the individual fiber before tensile tests, supporting paperboards were used to one side of the tensile specimens and were removed just before tensile tests.

2.5. DTA–TG analysis

To obtain an overview of mass loss of the Cf/LAS composites, DTA–TG analysis was performed using a calorimeter (Netzsch STA 404) with Al_2O_3 crucibles in air. The samples were heated from room temperature to 1200 °C at a heating rate of 10 °C min^{-1}.

3. Results

3.1. Densification and crystallization behavior

The sintered densities (as a percentage of the theoretical densities) of the Cf/LAS composites are reported in Table 2. The relative densities of the composites are in the range of 94–97%. Hence, the composites could achieve good sintering densities at modest hot-pressing temperatures by using the processing route developed in this study.

To study the crystallization behavior, XRD patterns of Cf/LAS2 and Cf/LAS4 hot pressed at different temperatures are shown in Fig. 2. For the samples Cf/LAS2 and Cf/LAS4, β-eucryptite and β-spodumene appear as the only phase, respectively, and no other phases could be identified. For the composite powders sintered at 1350 °C for 24 h, the diffraction peaks from β-eucryptite and β-spodumene are sharp and no anomalous intensity changes could be observed for the strongest peaks (1 0 1) for β-eucryptite and (2 0 1) for β-spodumene. Therefore, the intensity of the strongest peaks of the composite powders

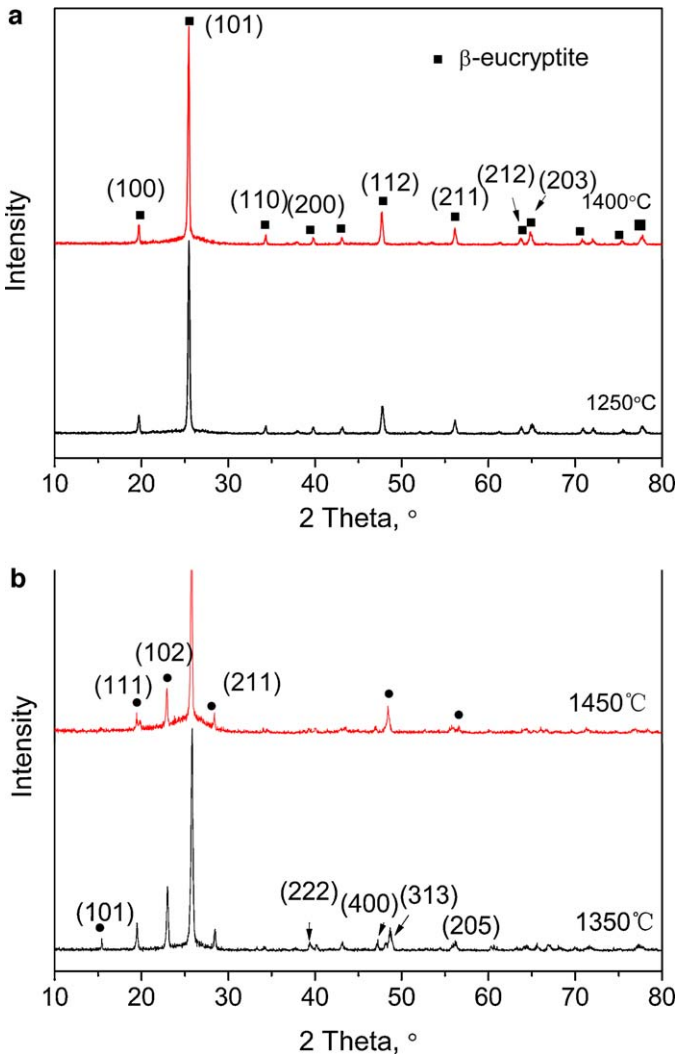

Fig. 2. XRD spectra of: (a) Cf/LAS2 and (b) Cf/LAS4 hot pressed at different temperatures.

sintered at 1350 °C for 24 h can be taken as a standard for comparing the relative crystallinity. The calculated amount of β-eucryptite and β-spodumene phases in the sintered bodies is determined by the integrated intensity of the strongest peak of the β-eucryptite and β-spodumene phases with a standard.[37] It indicates that no obvious increase of the relative crystallinity of β-eucryptite and β-spodumene occurs with increasing the sintering temperature, implying the near completion of crystalline process under such hot pressing conditions (Table 2).

Table 2
Sintered densities, crystal size and relative crystallinity of Cf/LAS composites hot pressed at different temperatures.

Materials	Hot pressing temperature (°C)	Relative density (%)	Average crystal size (μm)	Relative crystallinity (%)
Cf/LAS2	1250	91	0.5–2	80
	1350	95	–	76
	1400	95	1–2	88
Cf/LAS4	1350	97	1–2	56
	1400	96	–	49
	1450	96	1–2	62

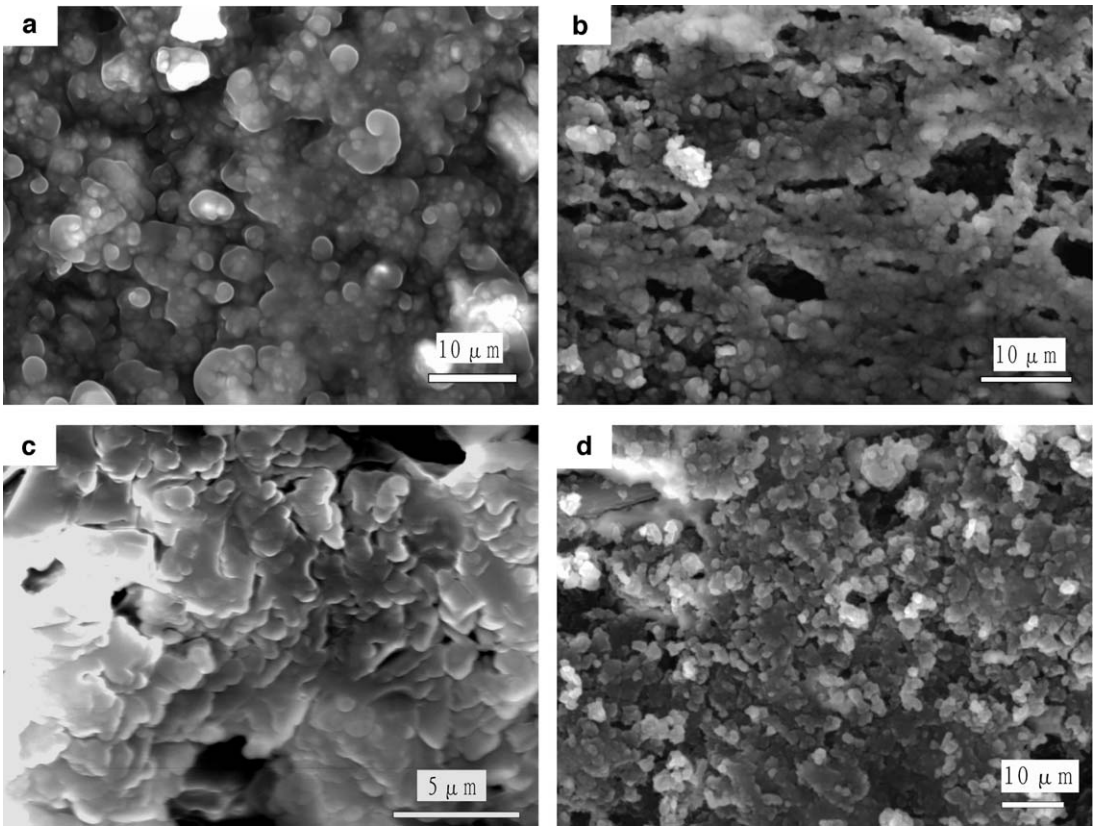

Fig. 3. SEM micrographs of etched surfaces of Cf/LAS2 hot pressed at: (a) 1250 °C, (b) 1400 °C and Cf/LAS4 hot pressed at (c) 1350 °C, (d) 1450 °C.

The size and morphology of β-eucryptite and β-spodumene crystals have no obvious change as the sintering temperature increased. The etched microstructures are composed of uniform and equiaxed crystal grains with a mean particle size of 1–2 μm (Fig. 3).

3.2. Flexural strength and fracture toughness

The mechanical properties of Cf/LAS2 composites are shown in Fig. 4a. Both the flexural strength and the fracture toughness increase with increasing temperature from 1250 °C to 1300 °C. The flexural strength and fracture toughness of Cf/LAS2 composites reach 571 ± 32 MPa and 9.8 ± 0.6 MPa $m^{1/2}$. On further increasing the sintering temperatures, the strength and toughness decrease. Especially for the sample of Cf/LAS2 hot pressed at 1400 °C, the strength and fracture toughness decrease drastically. As for the Cf/LAS4 composites, the flexural strength and fracture toughness have similar trend as the hot pressing temperature increases, reaching a maximum of 640 ± 72 MPa and 19.9 ± 1.8 MPa $m^{1/2}$ for sample hot pressed at 1400 °C, as compared to only 248 ± 44 MPa and 6.3 ± 1.0 MPa $m^{1/2}$ for Cf/LAS4 composite hot pressed at 1450 °C (Fig. 4b) respectively.

3.3. Morphologies of fractured surfaces

Fig. 5 shows fracture surface morphology of Cf/LAS composites hot-pressed at different temperatures. For the Cf/LAS2

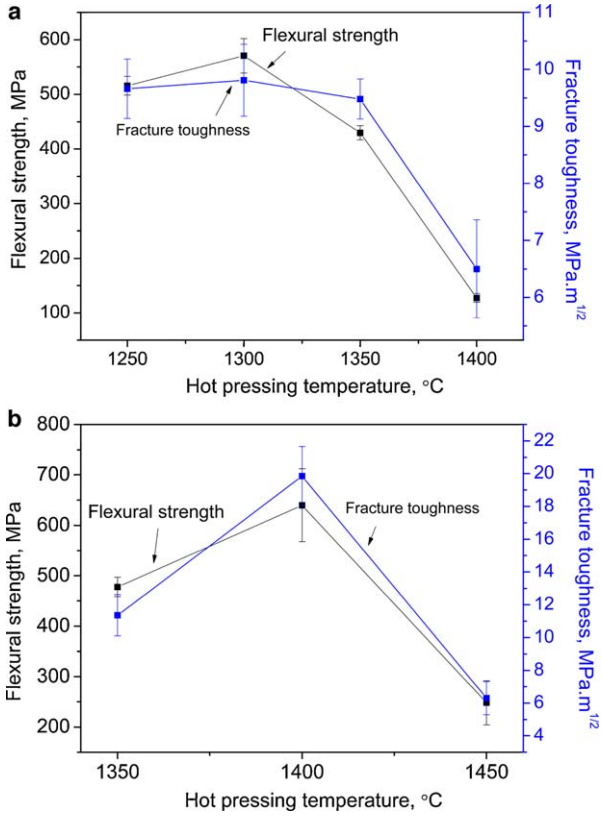

Fig. 4. Mechanical properties of: (a) Cf/LAS2 and (b) Cf/LAS4 composites as a function of hot pressing temperature.

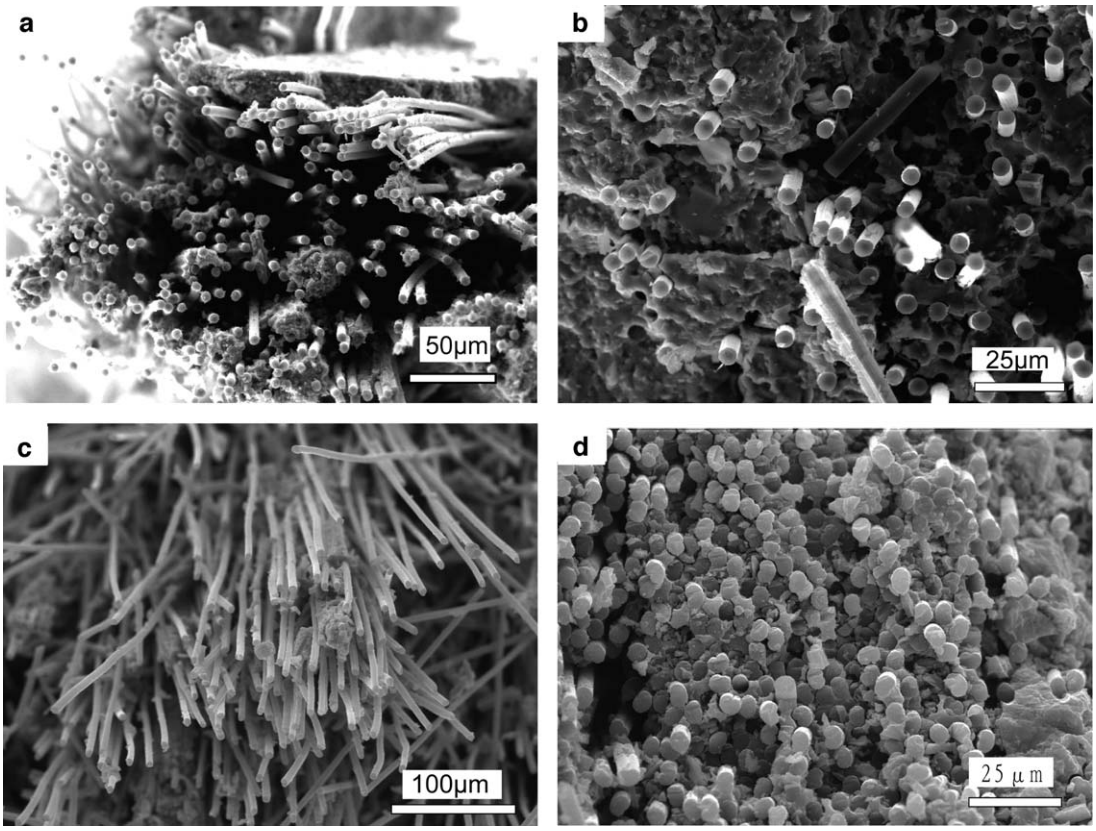

Fig. 5. Magnified micrographs of fracture surface of Cf/LAS2 hot pressed at: (a) 1300 °C, (b) 1400 °C and Cf/LAS4 hot pressed at (c) 1400 °C, (d) 1450 °C.

composite hot-pressed at 1300 °C and Cf/LAS4 composite hot-pressed at 1400 °C, large fiber pull-out is observed on the fracture surface (Fig. 5a and c). This indicates that the reinforcing effect of Cf is significant and the continuous fibers play an important role in carrying the load. Fiber pull-out is also found on the fracture surface of Cf/LAS2 composites hot-pressed at 1400 °C, however, the pull-out length is far shorter than that of Cf/LAS2 composites hot-pressed at 1300 °C and Cf/LAS4 composites hot-pressed at 1400 °C (Fig. 5b). For Cf/LAS4 composites hot-pressed at 1450 °C, the fracture surface is very flat and no fiber pull-out could be observed (Fig. 5d).

3.4. Interface characterization

HRTEM observations of the fiber/matrix interface reveal that different interfaces form at different hot pressing temperatures. For the Cf/LAS2 hot pressed at 1300 °C and Cf/LAS4 hot pressed at 1400 °C, the continuous interface demonstrates brick pattern characteristics at low magnification (Figs. 6a and 7a). At high magnification, very small cracks can be seen between the brick pattern. SAED results suggest that the interface exhibits a typical turbostratic structure, where the aromatic planes align within a little angle of the fiber axis (Figs. 6b and 7b). The similar interfacial structures were also founded in the SiC/LAS composite, in which turbostratic carbon layer formed between transition layer and matrix.[38,39] The chemical composition of interface of Cf/LAS2 hot pressed at 1300 °C has been determined by local EDX analysis. The result shows that the interfacial layer is enriched by carbon and some amount of O and Si (Fig. 6e).

For the Cf/LAS2 hot pressed at 1400 °C and Cf/LAS4 hot pressed at 1450 °C, the interfaces of the longitudinal section of fibers are sharp and regular, in comparison to that of the samples hot pressed at 1300 °C and 1400 °C (Figs. 6c and 7c). At high magnification, the surface is wavy, with amplitude which reaches 10 nanometers or so. The SAED pattern of the interface is obtained in the fiber periphery area. The continuous ring pattern is the characteristic of equiaxed {0 0 0 2} carbon planes (Fig. 7d). The EDX results show that aluminium, silicon and oxygen from the matrix have diffused into fibers and some amount of carbon also escape from fibers and diffuse into the neighboring matrix (Fig. 8).

3.5. Thermal stability

Thermal stability of Cf composites is necessary for many applications. A TG curve of Cf/LAS composites is shown in Fig. 9a. A sudden drop in the mass of the samples indicates carbon fibers start to be oxidized at 600 °C in air, corresponding to an exothermic peak (Fig. 9b). The oxidization of carbon fibers breaks down the fiber structure. Inevitably, the mechanical properties degrade when the Cf/LAS composites are used at 600 °C or higher.

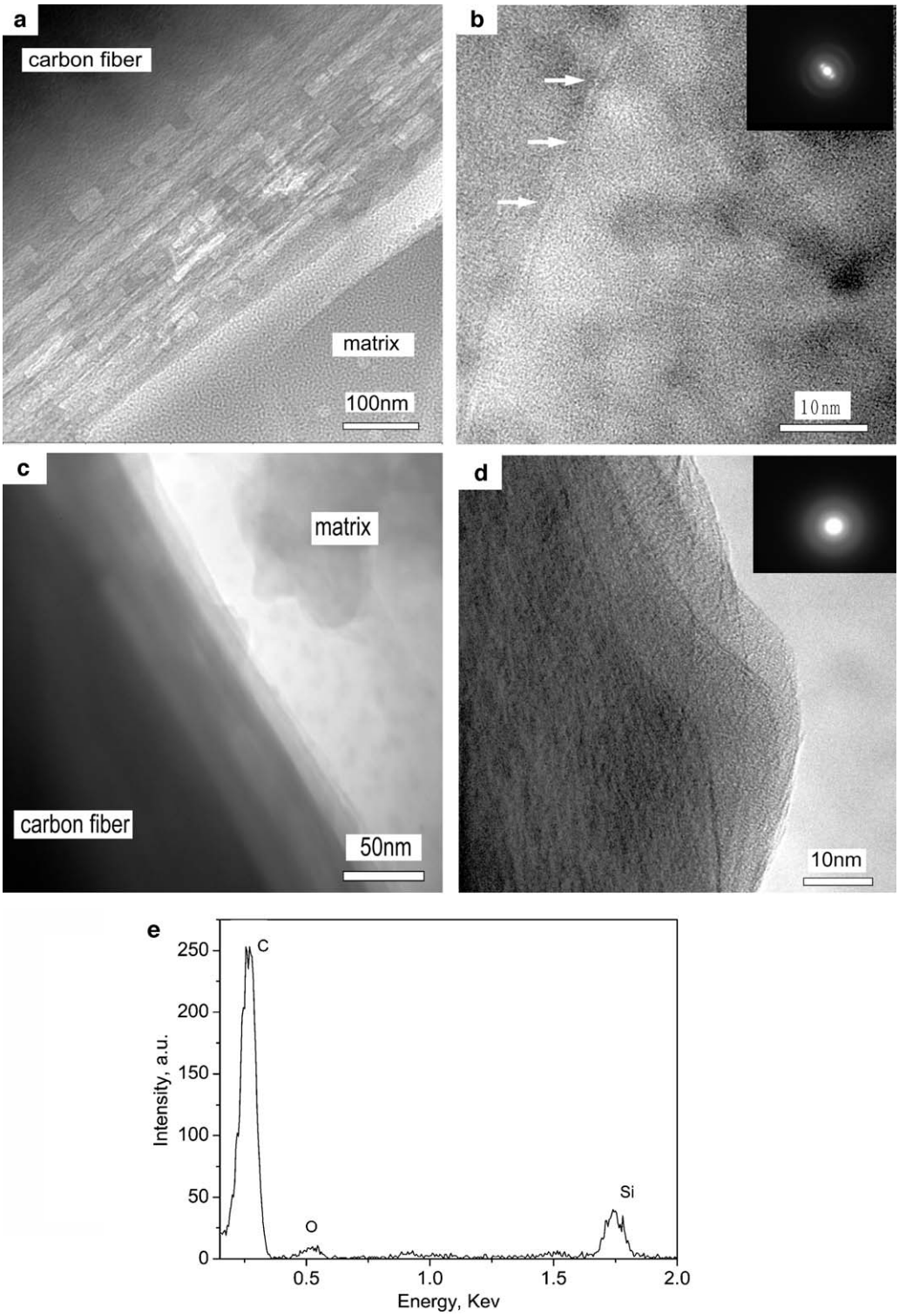

Fig. 6. TEM micrograph of Cf/LAS2 composite hot pressed at (a) 1300 °C, (c) 1400 °C; (b) and (d) corresponding to high resolution micrographs of interface of (a) and (c) photographs; (e) EDX of the interfacial layer between fiber and matrix in Fig. 4a.

4. Discussion

4.1. The formation of interface

TEM studies have revealed a carbon-rich layer with brick pattern microstructure in the composites hot pressed at relative lower temperatures. Despite of a large amount of carbon, trace amount of O and Si are also found in the interface area under such hot pressing condition. Cooper and Chyung et al.[40] studied the interfacial layer formation in SiC/LAS and SiC/CAS composites. They reported that a carbon-rich reaction layer was observed in all composites. The carbon layer is limited by the

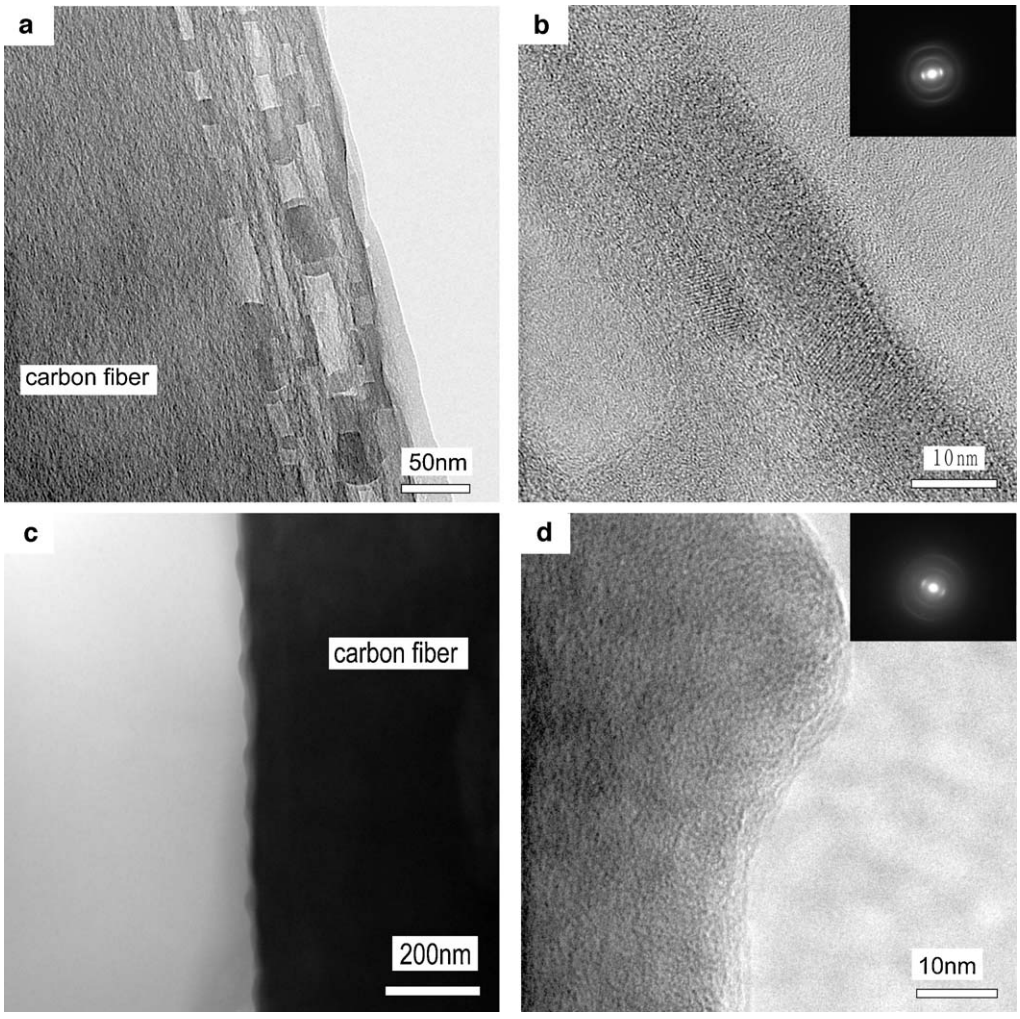

Fig. 7. TEM micrograph of Cf/LAS4 composite hot pressed at (a) 1400 °C, (c) 1450 °C. (b) and (d) corresponding to high resolution micrographs of interface of (a) and (c) photographs.

diffusion of silica from the fiber to the matrix. In the present study, the activities of Li, O, Al and Si also play an important role in control of the interface formation. The diffusion of Li, O, Al and Si from matrix to carbon fiber is attributed to the gradient between the carbon fibers and LAS matrix. The carbon fiber is categorized into the large family of turbostratic carbons, where some basic structural unit organizes in microfibrils along the fiber axis at the fiber surface.[41] The intrusive Li, O, Al and Si react with carbon in the carbon fiber, leading to the breakdown of the microfibrils. The reaction of C and O also causes the formation of microcrack in the interfacial layer (Fig. 6b). As a consequence, the discontinuous microfibrils demonstrate brick pattern characteristics.

The diffusion of Li, O, Al and Si accelerate with the increase of the hot pressing temperature. At relatively high temperatures, such as 1400 °C for Cf/LAS2 and 1450 °C for Cf/LAS4, sufficient Li, O, Al and Si diffuse into the carbon fiber and the microfibrils are decomposed totally. Carbon of decomposed microfibrils reacts with oxygen and the resultants flee during the sintering process. The residual carbon diffuses into matrix. This interdiffusion process leads to the formation of strong interface.

It has been evidenced that low-aromaticity carbon species are preferentially attacked by molten lithium/sodium nitrate.[42] Considering this conclusion, the phenomenon that brick-pattern interface of Cf/LAS4 occurs at higher temperature compared with that of Cf/LAS2 is due to the lower lithium concentration of the Cf/LAS4.

The residual tensile strength of carbon fibers is 1710 MPa for Cf/LAS2 hot pressed at 1400 °C, decreased significantly compared with 2715 MPa for Cf/LAS2 hot pressed at 1250 °C (Fig. 10). This experimental data support the EDX results that the elements of matrix Cf/LAS2 hot pressed at 1400 °C invade into fibers severely, leading to the reduction of carbon tensile strength and formation of strong interface. Similar results are also observed in the Cf/LAS4 composites.

4.2. The effect of thermal mismatch

Thermal mismatch in continuous carbon fiber reinforced lithium aluminosilicate glass ceramics matrix composites should be considered both from the radial and axial directions because carbon fibers exhibit anisotropic thermal properties. The radial

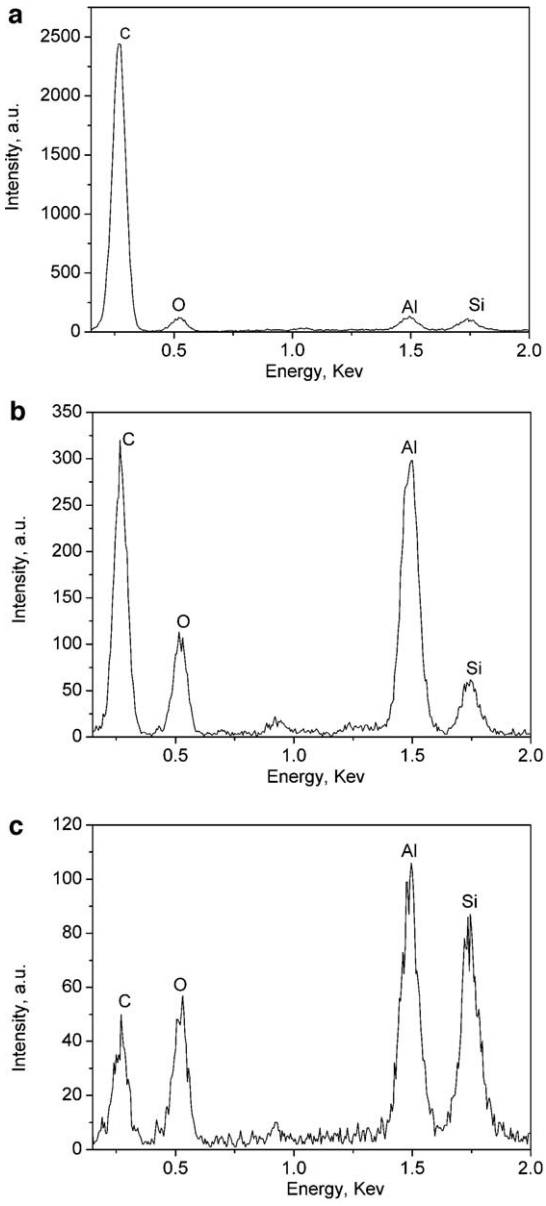

Fig. 8. EDX spectra of Cf/LAS2 composite hot pressed 1400 °C taken: (a) at the fiber surface (at 100 nm from the interface); (b) in the interface; (c) at the matrix near the interface.

thermal expansion coefficient of carbon fibers between room temperature and 900 °C is about $8 \times 10^{-6}\,°C^{-1}$,[43] which is larger than that of the β-eucryptite (-64 to $-86 \times 10^{-7}\,°C^{-1}$) and β-spodumene ($+9$–$12 \times 10^{-7}\,°C^{-1}$) matrix.[44,45] The matrices are subjected compressive stress, which is beneficial to the formation of weak interfacial bonding. On the other hand, the axial CTE of carbon fibers is approximately zero due to the specific orientation of graphite grain. Consequently, β-spodumene matrix of Cf/LAS4 is subjected less residual thermal stress than that of β-eucryptite matrix of Cf/LAS2 since the β-spodumene phase has similar CTE with the axial of carbon fibers. This would be responsible for the higher mechanical performance of Cf/LAS4 than that of Cf/LAS2 in certain temperature range.

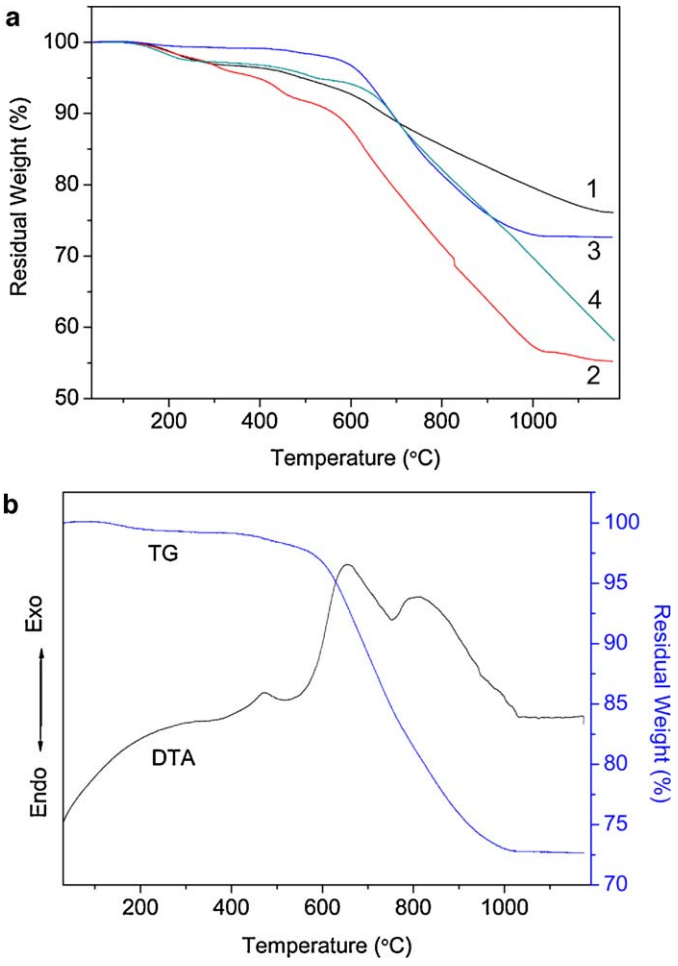

Fig. 9. (a) TG curves of Cf/LAS2 hot pressed at (1) 1250 °C, (2) 1400 °C and Cf/LAS4 hot pressed at (3) 1350 °C, (4) 1450 °C and (b) DTA–TG curves of Cf/LAS4 hot pressed at 1350 °C.

4.3. Relationship between interface and mechanical properties

The toughening effect of fibers in a ceramic matrix composite depends both on the nature of the interface between fibers and matrix and on the retained strength of the fibers after hot pressing.[46–48] The nature of the interface is governed by the processing conditions as well as the starting materials for the matrix and the type of reinforcing fibers. These factors can significantly affect the interfacial strength and may lead to the formation of the preferred state of a relatively weak interface.[36,49]

The SAED results show that the interfaces of Cf/LAS2 hot pressed at 1300 °C and Cf/LAS4 hot pressed at 1400 °C have turbostratic structures. The brick pattern structure acts as a mechanical fuse, which promotes crack deflection and interface sliding. As for the crack deflection, the interfacial part exhibits microcrack morphology, where the discontinuous microfibrils align long the fiber axis. Such a structure is very suitable to promote crack branching on the disclinations as well as crack deflection. Another beneficial point to enhance the mechanical properties is that the brick pattern structure can promote the interface sliding. When submitted to overload stresses, the

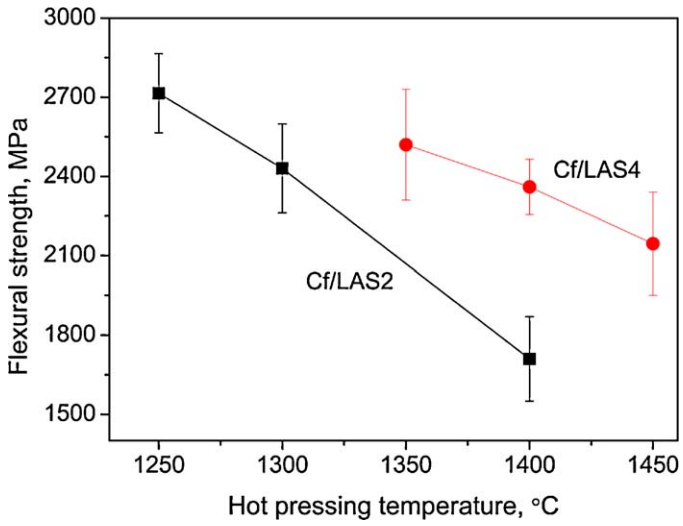

Fig. 10. Residual flexural strength of carbon fibers of Cf/LAS composites hot pressed at different temperatures.

carbon fiber can debond from the matrix easily due to the brick pattern structure of the interface. The fracture toughness increases because the fracture energy can be absorbed during the process of crack splitting and crack deflection. The maximum flexural strength and fracture toughness reach 571 ± 32 MPa and 9.8 ± 0.6 MPa $m^{1/2}$ for Cf/LAS2 composites and 640 ± 72 MPa and 19.9 ± 1.8 MPa $m^{1/2}$ for Cf/LAS4 composites, respectively. Shin et al.[50] prepared Nicalon-SiC fibers reinforced (35 vol.%) LAS glass–ceramics composites by a slurry infiltration and hot pressing method. The ultimate strength and elastic modulus of the as-fabricated composites, as determined by four-point flexural tests, are 550 MPa and 130 GPa. Kim et al.[9] studied the mechanical properties of SiC fibers reinforced (35 vol.%) LAS glass–ceramics composites fabricated by sol–gel method. They found that the fracture toughness increases from 11 MPa $m^{1/2}$ for the undoped composite to 16 MPa $m^{1/2}$ for the 5 wt% doped composites. Prewo[51] investigated room temperature and high temperature mechanical properties of SiC fibers reinforced (35 vol.%) LAS glass–ceramics composites prepared by slurry infiltration and hot pressing method. The ultimate tensile strength at 22 °C was nearly 700 MPa and the failure strain was 1%. Zhien[29] studied the effect of fiber content, hot pressing temperature and pressure on the mechanical properties of Cf/LAS composites. The flexural strength and fracture toughness approach 646 MPa and 20.1 MPa $m^{1/2}$ respectively. Although SiC fibers and carbon fibers have similar tensile strength, it is difficult to compare the mechanical properties in this study with others due to the different test methods and experimental parameters. The flexural strength of Shin et al.'s specimens was measured using four-point flexural test. The size of specimens was 1.7 mm × 3 mm × 60 mm. The span of the testing apparatus of 15 mm, and a crosshead speed of 0.5 mm min^{-1} was used. In the current study, however, the specimens were 3 mm × 4 mm × 36 mm, with a span of 30 mm and a crosshead speed of 0.5 mm min^{-1}.

For Cf/LAS2 hot pressed at 1400 °C and Cf/LAS4 hot pressed at 1450 °C, brick pattern structure is consumed during active chemical diffusion process, leading to the formation of strong fiber/matrix interfacial bonding. Therefore, with increasing hot pressing temperature, the fiber pull-out length becomes shorter, or even no fiber pull-out is observed. As a result, the composite exhibits brittle fracture behavior.

5. Conclusions

Uni-Cf/LAS composites were prepared by sol–gel and hot-pressing method. A flexural strength of 571 ± 32 MPa and fracture toughness of 9.8 ± 0.6 MPa $m^{1/2}$ parallel to the fiber direction for the uni-Cf/LAS2 composite hot-pressed at 1300 °C and flexural strength of 640 ± 72 MPa and fracture toughness of 19.9 ± 1.8 MPa $m^{1/2}$ for the uni-Cf/LAS4 composite hot-pressed at 1400 °C are attributed to the fiber pull-out. The thin interfacial layer with brick pattern charateristics of Cf/LAS2 and Cf/LAS4 hot pressed at lower temperatures acts as a mechanical fuse with very low interfacial debonding energy values, so the composite exhibited "toughness" behavior. But for the Cf/LAS2 composite hot-pressed at 1400 °C and Cf/LAS4 composite hot-pressed at 1450 °C, the chemical bond results in strong interface between fiber and matrix, so the composites show "brittle" behavior.

Acknowledgements

This work is supported by National Natural Science Foundation of China (NSFC, Grant No. 51021002) and National Natural Science Foundation of China (Grant No. 50672018) and National High-tech R&D Program (863 Program) (Grant No. 2007AA03Z340).

References

1. Lichtenstein AI, Jones RO, De Gironcoli S, Baroni S. Anisotropic thermal expansion in silicates: a density functional study of β-eucryptite and related materials. *Phys Rev B* 2000;**62**(17):11487–93.
2. Karmakar B, Kundu P, Jana S, Dwivedi RN. Crystallization kinetics and mechanism of low-expansion lithium aluminosilicate glass–ceramics by dilatometry. *J Am Ceram Soc* 2002;**85**(10):2572–4.
3. Lin MH, Wang MC. Crystallization behavior of β-spodumene in the calcinations of Li_2O–Al_2O_3–SiO_2–ZrO_2 gels. *J Mater Sci* 1995;**30**(10):2716–21.
4. Suzuki H, Takahashi J, Saito H. Preparation and crystallization of precursor powders in Li_2O–Al_2O_3–SiO_2 system. *Chem Soc Jpn* 1991;**10**:1312–8.
5. Villalobos GR, Speyer RF. Electrical resistance as a tool in determining the failure of fibres in a nicalon-reinforced LAS glass–ceramic with Ta_2O_5 additions. *J Mater Sci* 1997;**32**(21):5577–81.
6. DrissiHabti M. Assessment of the mechanical behaviour of SiC fibre reinforced magnesium lithium aluminosilicate glass–ceramic matrix composite tested under uniaxial tensile loading. *J Eur Ceram Soc* 1997;**17**(1):33–9.
7. Hasselman DPH, Donaldson KY, Thomas JR. Thermal conductivity of vapor liquid solid and vapor solid silicon carbide whisker-reinforced lithiumaluminosilicate glass ceramic composites. *J Am Ceram Soc* 1996;**79**(3):742–8.
8. Fox AG, Hunt RK, Maldia LC. Hot sodium sulphate corrosion of a Nicalon silicon carbide fibre-reinforced lithium aluminosilicate glass–ceramic matrix composite. *J Mater Sci* 1995;**30**(24):6161–70.
9. Kim KS, Jang HM, Baik YK. SiC fiber-reinforced lithium aluminosilicate matrix composites fabricated by the sol–gel process. *J Mater Sci* 1995;**30**(4):1009–17.

10. Prewo KM, Brennan JJ, Layden GK. Fiber reinforced glasses and glass–ceramics for high performance applications. *Ceram Bull* 1986;**65**(2):305–13.
11. Phillips DC, Sambell RA, Bowen D. The mechanical properties of carbon fiber reinforced Pyrex glass. *J Mater Sci* 1972;**7**:1454–64.
12. Sambell RA, Bowen DH, Phillips DC. Carbon fiber composites with ceramic and glass matrices. *J Mater Sci* 1972;**7**:676–81.
13. Phillips DC. Interfacial bonding and the toughness of carbon fiber reinforced glass and glass–ceramics. *J Mater Sci* 1974;**9**:1847–54.
14. Poowancum A, Matsumaru K, Ishizaki K. Development of low-thermal-expansion silicon carbide/zirconium tungstate porous ceramics. *J Am Ceram Soc* 2010;**93**(10):2978–80.
15. Kanamori K, Kineri T, Fukuda R, Kawano T, Nishio K. Low-temperature sintering of ZrW(2)O(8)–SiO(2) by spark plasma sintering. *J Mater Sci* 2009;**44**(3):855–60.
16. Ogiwara T, Noda Y, Shoji K, Kimuray O. Low-temperature sintering of high-strength beta-eucryptite ceramics with low thermal expansion using Li(2)O–GeO(2) as a sintering additive. *J Am Ceram Soc* 2011;**94**(5):1427–33.
17. Garcia-Moreno O, Fernandez A, Torrecillas R. Solid state sintering of very low and negative thermal expansion ceramics by spark plasma sintering. *Ceram Int* 2011;**37**(3):1079–83.
18. Reveron H, Blanchard L, Vitupier Y, Riviere E, Bonnefont G, Fantozzi G. Spark plasma sintering of fine alpha-silicon nitride ceramics with LAS for spatial applications. *J Eur Ceram Soc* 2011;**31**(4):645–52.
19. Sheppard LM. Enhancing performance of ceramic composites. *Am Ceram Soc Bull* 1992;**71**:617–9.
20. Cornie JA, Chiang YM, Uhlmann DR. Processing of metal and ceramic matrix composites. *Am Ceram Soc Bull* 1986;**65**(2):293–304.
21. Arvind A, Sarkar A, Shrikhande VK, Tyagi AK, Kothiyal GP. The effect of TiO_2 addition on the crystallization and phase formation in lithium aluminum silicate (LAS) glasses nucleated by P_2O_5. *J Phys Chem Solids* 2008;**69**:2622–7.
22. Alekseeva I, Dymshits O, Ermakov V, Zhilin A, Petrov V, Tsenter M. Raman spectroscopy quantifying the composition of stuffed β-quartz derivative phases in lithium aluminosilicate glass–ceramics. *J Non-Cryst Solids* 2008;**354**:4932–9.
23. Hu AM, Li M, Mao DL. Growth behavior, morphology and properties of lithium aluminosilicate glass ceramics with different amount of CaO, MgO and TiO_2 additive. *Ceram Int* 2008;**34**:1393–7.
24. Guo XZ, Yang H, Han C, Song FF. Nucleation of lithium aluminosilicate glass containing complex nucleation agent. *Ceram Int* 2007;**33**:1375–9.
25. Zheng WH, Cheng JS, Tang LY, Quan J, Cao X. Effect of Y_2O_3 addition on viscosity and crystallization of the lithium aluminosilicate glasses. *Thermochim Acta* 2007;**456**:69–74.
26. Bae SJ, Kang U, Dymshits O, Shashkin A, Tsenter M, Zhilin A. Raman spectroscopy study of phase transformations in titania-containing lithium aluminosilicate glasses doped with CoO. *J Non-Cryst Solids* 2005;**351**:2969–78.
27. Xia L, Wen GW, Song L, Wang XY. The crystallization behavior and thermal expansion properties of β-eucryptite prepared by sol–gel route. *Mater Chem Phys* 2010;**119**:495–8.
28. Xia L, Wen GW, Song L, Wang XY. Sol–gel synthesis and crystallization behaviour of beta-spodumene. *J Sol–Gel Sci Tech* 2009;**52**:134–9.
29. Liu ZE, Yuan JJ, Xue ZY. The interface, microstructure and mechanical properties of Cf/LAS glass–ceramic composites. *J Mater Sci* 1995;**30**:399–404.
30. Hardy AB, Gowda G, McMahon TJ, Riman RE, Rhine WE, Bowen HK. Ultrastructure processing of advanced ceramics. New York: Wiley; 1988.
31. Xia L, Wen GW, Song L, Wang XY. The effect of aluminum sources on synthesis of low expansion glass–ceramics in lithia–alumina–silica system by sol–gel route. *J Non-Cryst Solids* 2009;**355**:2349–54.
32. Bansal NP, Eldridge JI. Effects of interface modification on mechanical behavior of Hi-Nicalon fiber-reinforced Celsian matrix composites. *Ceram Eng Sci Proc* 1997;**18**(3):379–89.
33. Beesley CP. The applications of CMCs in high integrity gas turbine engine. *Key Eng Mat* 1997;**127-131**:165–74.
34. Benson PM, Spear KE, Pantano CG. Interfacial characterization of glass/Nicalon fiber composites: a thermodynamic approach. *Ceram Eng Sci Proc* 1988;**9**:663–70.
35. Bleay SM, Scott VD, Harris B, Cooke RG, Habib FA. Interface characterization and fracture of calcium aluminosilicate glass–ceramic reinforced with Nicalon fibres. *J Mater Sci* 1992;**27**:2811–22.
36. Bonney LA, Cooper RF. Reaction–layer interfaces in SiC-fiberreinforced glass–ceramics: a high resolution scanning transmission electron microscopy study. *J Am Ceram Soc* 1990;**73**(10):2916–21.
37. Wang MC, Yang S, Wen SB, Wu NC. Sintering Li_2O–Al_2O_3–$4SiO_2$ precursor powders with ultrafine TiO_2 additives. *Mater Chem Phys* 2002;**76**:162–70.
38. Lancin M, Ponthieu, Marhic C, Miloche M. SIMS, EDX, EELS, AES, XPS study of interphases in Nicalon fibre-LAS glass matrix composites, Part I. Composition of the interphases. *J Mater Sci* 1994;**29**: 3759–66.
39. Ponthieu C, Marhic C, Lancin M, Herbots N. SIMS, EDX, EELS, AES, XPS study of interphases in Nicalon fibre-LAS glass matrix composites, Part II. Chemistry of the interphases. *J Mater Sci* 1994;**29**: 4535–44.
40. Cooper RF, Chyung K. Structure and chemistry of the fibrematrix interfaces in silicon carbide fibre-reinforced glass–ceramic composites: an electron microscopy study. *J Mater Sci* 1987;**22**:3148–60.
41. Lancin M, Marhic C. TEM study of carbon fiber reinforced aluminium matrix composites: influence of brittle phases and interface on the mechanical properties. *J Eur Ceram Soc* 2000;**20**:1493–503.
42. Havel M, Colomban P. Skin/bulk nanostructure and corrosion of SiC-based fibres: a surface Rayleigh and Raman study. *J Raman Spectrosc* 2003;**34**:786–94.
43. Watt W, Perov BW. Strong fibers. In: Kelly A, Rabotnov YN, editors. *Handbook of composites*. Amsterdam: Elsevier Science Publishing Company Inc.; 1985. p. 436–7.
44. Roy R, Agrawal DK, Mckinstry HA. Very low thermal expansion coefficient materials. *Annu Rev Mater Sci* 1989;**19**:59–81.
45. Strand Z. Glass–ceramic materials: glass science & technology. New York: Elsevier Science Publishing Company Inc.; 1986.
46. Rice RW. Ceramic matrix composite toughening mechanisms: an update. *Ceram Eng Sci Proc* 1985;**6**(7–8):589–607.
47. Kerans RJ, Hay RS, Pagano NJ. The role of the fiber–matrix interface in ceramic composites. *Am Ceram Soc Bull* 1989;**68**(2):429–42.
48. Thouless MD, Sbaizero O, Sigl LS, Evans AG. Effect of interface mechanical properties on pullout in a SiC-fiber-reinforced lithium aluminum silicate glass–ceramic. *J Am Ceram Soc* 1989;**72**(4):525–32.
49. Mouchon E, Colomban P. Oxide ceramic matrix/oxide fibre woven fabric composites exhibiting dissipative fracture behaviour. *Composites* 1995;**26**(3):175–82.
50. Shin HH, Speyer RF. Effect of hot pressing time and post-heat treatment on the microstructure and mechanical properties of SiC-fiber-reinforced glass–ceramics composites. *J Mater Sci* 1994;**29**:3630–6.
51. Prewo KM. Tensile and flexural strength of silicon carbide fiber-reinforced glass–cermics. *J Mater Sci* 1986;**21**:3590–600.